Comparative Properties of a Three-Dimensional Model of *Plasmodium falciparum* Ornithine Decarboxylase

L. Birkholtz, F. Joubert, A.W.H. Neitz, and A.I. Louw*

Department of Biochemistry, School of Biological Sciences, Faculty of Natural and Agricultural Sciences, University of Pretoria, Pretoria, South Africa

ABSTRACT **The ornithine decarboxylase (ODC) component of the bifunctional S-adenosylmethionine decarboxylase/ornithine decarboxylase enzyme (PfAdoMetDC-ODC) of *Plasmodium falciparum* was modeled on the crystal structure of the *Trypanosoma brucei* enzyme. The homology model predicts a doughnut-shaped active homodimer that associates in a head-to-tail manner. The monomers contain two distinct domains, an N-terminal α/β-barrel and a C-terminal modified Greek-key domain. These domains are structurally conserved between eukaryotic ODC enzymes and are preserved in distant analogs such as alanine racemase and triosephosphate isomerase-like proteins. Superimposition of the PfODC model on the crystal structure of the human enzyme indicates a significant degree of deviation in the carbon α-backbone of the solvent accessible loops. The surface locality of the ab initio modeled 38 amino acid parasite-specific insert suggests a role in the stabilization of the large bifunctional protein complex. The active site pockets of PfODC at the interface between the monomers appear to be conserved regarding the binding sites of the cofactor and substrate, but each contains five additional malaria-specific residues. The predicted PfODC homology model is consistent with mutagenesis results and biochemical studies concerning the active site residues and areas involved in stabilizing the dimeric form of the protein. Two competitive inhibitors of PfODC could be shown to interact with several parasite-specific residues in comparison with their interaction with the human ODC. The PfODC homology model contributes toward a structure-based approach for the design of novel malaria-specific inhibitors. Proteins 2003;50:464–473.**

Key words: homology model; malaria; ornithine decarboxylase; polyamines

INTRODUCTION

Polyamines are ubiquitous cationic molecules that are essential for cell growth and differentiation.[1] Ornithine, an intermediate of the urea cycle, is decarboxylated by ornithine decarboxylase (ODC, EC: 4.1.1.17) to produce putrescine. Addition of aminopropyl groups donated by decarboxylated S-adenosylmethionine produces spermidine and spermine.[1] ODC and S-adenosylmethionine decarboxylase (AdoMetDC, EC: 4.1.1.50) regulate polyamine metabolism, and inhibitors against these enzymes have been shown to block polyamine biosynthesis. This information is being applied in diverse therapies ranging from tumor suppressors to antiparasitic agents.[2–4] Specifically, the ODC inhibitor, α-difluoromethylornithine (DFMO), is currently used in the treatment of African sleeping sickness (*Trypanosoma gambiense*). A global resistance of *Plasmodium falciparum*, the etiologic agent of malaria, against most known and cost-effective drugs underscores the need for the characterization of novel antimalarial targets and drugs. Inhibition of ODC in the malaria parasite with DFMO or AdoMetDC with MDL73811 has been shown to lead to erythrocytic schizogony arrest in vitro and to be curative of rodent malaria when used in combination with polyamine analogs such as bis(benzyl)-polyamines.[5–9] These results provide strong support for studies aimed at the characterization of enzymes of the polyamine pathway of the parasite to evaluate their potential as antimalarial targets.

The normally independent decarboxylases of other organisms have been shown to occur as a large bifunctional protein complex in *P. falciparum* with a predicted molecular mass of ~330 kDa (PfAdoMetDC-ODC).[10] The AdoMetDC component is located at the N-terminus and linked to ODC by ~180 amino acid residues. ODC is a pyridoxal-5′-phosphate (PLP)-dependent enzyme that catalyzes the decarboxylation of L-ornithine to putrescine. It has been extensively studied in other organisms to clarify its extremely short half-life and regulatory mechanism. Eukaryotic ODC occurs as a dimer of identical subunits of about 50 kDa each and is distinct from bacterial ODCs.[11] The two active sites are formed at the interface between the monomers and consist of residues donated by both monomers (murine enzyme numbering Lys_{69}, Lys_{169}, His_{197} on one subunit and Cys_{360} on the other).[1,11] The malarial ODC (PfODC) shares the consensus areas of the other ODCs, and the active site residues are also conserved.[10] However, both decarboxylases of the

Grant sponsor: South African National Research Foundation; Grant sponsor: Medical Research Council of South Africa; Grant sponsor: University of Pretoria.

*Correspondence to: Abraham I. Louw, Department of Biochemistry, University of Pretoria, Pretoria, South Africa 0002. E-mail: braam.louw@bioagric.up.ac.za

Received 23 April 2002; Accepted 26 July 2002

PfAdoMetDC-ODC complex contain inserted amino acids compared with other organisms. The functions of these unique inserts are unknown.

Structural data are available for the murine, human, *T. brucei*, and *Lactobacillus* ODC enzymes[12–16] and for the human AdoMetDC enzyme[17] but not for the malarial enzymes. Detailed knowledge of the structure and function of the individual enzymes is required to clarify and understand their arrangement and interactions in the unique bifunctional complex. X-ray crystallography and NMR spectroscopy are the preferred methods to obtain detailed structural information of proteins, but both methods require large quantities of protein. The high A+T content of the parasite genome contributes in many instances to the low or insignificant expression of protein from heterologous systems.[18,19] Furthermore, crystallization of malarial proteins is problematic because of the characteristic prevalence of regions of low complexity and/or inserted amino acids, as evidenced by the paucity of protein crystal structures. Comparisons between various proteins have shown that their tertiary structures are usually better conserved in evolution than their amino acid sequences.[20] This information has resulted in the application of homology modeling as an additional and/or alternative method to obtain protein structural information.[20] No crystal structure could be obtained yet for malarial dihydrofolate reductase (DHFR) notwithstanding its widespread resistance to antifolates and importance as a selective and validated antimalarial drug target. Malarial DHFR also occurs in a bifunctional complex with thymidilate synthase and contains inserted amino acids.[21,22] The mechanism of resistance of DHFR to known antimalarials could be explained by a homology model and furthermore led to the discovery of lead inhibitors.[21–24] The extent of sequence identity between ODCs from a variety of species and the malarial ODC protein suggested the feasibility of a similar comparative protein structure modeling approach for the generation of its three-dimensional structure. Here we report a homology model of PfODC and some structural analyses that could contribute toward the design of inhibitors specifically targeted against this enzyme in *P. falciparum*.

MATERIALS AND METHODS

Comparative Modeling of Monomeric PfODC

Multiple pairwise alignment (CLUSTALX)[25] was used to compare the PfODC amino acid sequence (GenBank Accession Number AF094833) with those of *Leishmania donovani* (GenBank Accession Number M81192), *Mus musculus* (GenBank Accession Number J03733), *Homo sapiens* (GenBank Accession Number M31061), and *Trypanosoma brucei* (GenBank Accession Number J02771). The malaria-specific insert (residues 1139–1296, PfAdoMetDC-ODC numbering) and the hinge region (residues 573–837) were removed from the PfODC sequence because of the absence of the corresponding sequence in the modeling template. The remaining 411 residues (838–1138/1297–1406) of the ODC component were submitted to the SWISS-Model server (Automated Protein Modeling Server, Version 3.5, GlaxoWellcome Experimental Research, Geneva, Switzerland)[26–28] for comparative protein structure modeling by rigid-body assembly with the following knowledge-based approach.[29–32] Suitable templates on which to base the model were found by searching all similarities within the target sequence compared with sequences of known structures with use of BLASTP2 searches of the ExNRL-3D database.[2] Templates with sequence identity above 25% and larger than 20 residues were selected by SIM and used to detect domains that could be modeled based on unrelated templates.[33] ProModII* was subsequently used to generate models using ExPDB.[3] Energy minimization and structure refinement were performed with GROMOS96 to reduce steric overlap specifically in side-chains (default parameters using steepest gradient for 200 cycles with Gromos96 force field, BIOMOS b.v. Company). The resulting model was then validated manually with the WHAT_CHECK module of the WHAT IF program (version 19970813-1517)[34] and with the PROCheck program.[35] Molecular surfaces and potentials were created with GRASP (Graphical Representation and Analyses of Structural Properties, Columbia University, New York, NY).[36] Models were visualized and edited with SWISS-PDB† Viewer and analyzed with the InsightII package (Accelrys) on a Silicon Graphics Octane workstation. The SWISS-PDB Viewer scenes were rendered with PovRay. Servers used for classification of the PfODC structure include BLOCKS (http://www.blocks.fhcrc.org/), Pfam (http://pfam.wustl.edu/), CATH,[37] SCOP (Structural Classification of Proteins),[38] and DALI (http://www.ebi.ac.uk/dali/). Low complexity regions in PfODC were identified with the SEG Program.[39]

Dimerization of Monomeric PfODC

The dimeric form of PfODC was built by superimposing the PfODC monomers on the dimeric *T. brucei* crystal structure using the Improved fit module of SWISS-PDB Viewer and merging the coordinates into one planar field. The resulting dimeric PfODC was then subjected to energy minimization with the Discover3 module of the InsightII package (cff91 force field for 10,000 iterations with a conjugate gradient) and checked for any disallowed bumps occurring between the two different chains. Interacting residues were analyzed with Protein Explorer (http://www.umass.edu/microbio/chime/explorer) and LigPlot (Version4.0)[40] The structure was analyzed for quality with the WHAT_CHECK module of the WHAT IF program.[34]

Docking of Ligands Into the Active Site of Dimeric PfODC

Active site residues were identified as those corresponding to proven functional residues in the active site pockets of the *Trypanosoma* and human ODC crystal structures.[12,13,41,42] These include Lys_{69}, Arg_{154}, His_{197}, $Gly_{235-237}$, Glu_{274},

*SWISS-Model sequence database, reflecting the protein sequences of ExPDB.

†The structure database used by the SWISS-Model is derived from the Brookhaven Protein Data Bank (PDB, BNL).

Arg_{277}, Tyr_{389}, Asp_{332}, Cys_{360}, and Asp_{361} (numbers according to the *Trypanosoma* protein). Structures for the ligands bound to ODC (PLP, DFMO, and two competitive inhibitors CGP52622A and CGP54169A from Novartis Pharma)[39–41] were generated with the Builder module of the InsightII package, and their energies were minimized as described above. Binding of PLP and DFMO requires the formation of a Schiff-base between the two ligands with DFMO and then also forming a covalent bond to the S_γ atom of Cys_{360} (*T. brucei* numbering). To dock this transition state complex of PLP-DFMO into PfODC, we created the structure for the linked PLP-DFMO and formed a covalent link with Cys_{1355}. To analyze the binding of ornithine, a second transition state complex was created between PLP and ornithine and analyzed as for the PLP-DFMO ligands. The ligand-ODC complexes were then minimized as described above. Possible interactions between the ligands and residues in PfODC were analyzed with LigPlot.[40] The structures were analyzed for quality with the WHAT IF program.[34] The two competitive inhibitors, CGP52622A and CGP54169A (Novartis Pharma), are 3-amino-oxy-1-propanamine structural homologs. To analyze the possible interactions of these inhibitors in the active site pocket of PfODC, the structures were superimposed on the coordinates of the corresponding ligands minimized in the PfODC active site pocket (i.e., CGP52622A was superimposed on the location of the minimized PLP). Energy minimization was repeated for the ligand-ODC complexes as described above. The ligands were also analyzed for any bumps occurring between van der Waals radii. Possible interactions between the ligands and residues in ODC were analyzed with LigPlot and the interacting energies with the Docking module of InsightII.[40] The structures were analyzed for quality with the WHAT IF program.[34] The same procedure was followed for analyzing the binding of the CGP54169A and CGP52622A inhibitors into the human ODC active site pocket (PDB no. 1D7K).[12]

RESULTS AND DISCUSSION

Comparisons between homologous proteins have shown that conformations are better conserved in evolution than the corresponding amino acid sequences.[20] Analyses of the PfODC primary sequence with the BLOCKS and Pfam databases indicated that the malarial ODC, as all the other ODCs, belong to the group IV decarboxylase family of proteins. This family includes ornithine, arginine, and diaminopimelic acid decarboxylases, probably based on a shared function and similarity between substrates. However, the CATH database places ODC in a hierarchical fashion with the lyase homologous superfamily, which shares topologies, consisting of a barrel-like architecture, with lyases and thrombin. These proteins are grouped into the mainly β-single-domain class of proteins according to evolutionary and structural groupings. SCOP places ODC in a superfamily of PLP-binding proteins, which include the alanine racemase-like family, based on a triosephosphate isomerase (TIM) barrel-like fold. The α/β-barrel structure found in these proteins seems extremely well preserved even in distant homologs (alanine racemase and TIM proteins) with diverse functions. From the above, it is apparent that characteristic structural features are conserved in evolution even between proteins with diverse primary sequences.

Characterization of Monomeric PfODC

To apply homology modeling, the first nontrivial step is to obtain a multiple alignment of the query amino acid sequence against sequences from other known structures. Multiple alignment of the PfODC sequence with those of four other organisms indicated two areas where amino acids were uniquely inserted into the malaria sequence (residues 1047–1085 and 1139–1296) as well as the hinge region (residues 573–837). At present, there are no known homologs of the inserted or hinge region sequences. The largest insertion of 158 residues and the hinge region were thus removed to arrive at a satisfactory homology model. Subsequent pairwise alignment of the remaining 411 residues of PfODC showed the highest identity to the amino acid sequences of the *T. brucei* enzymes (41.54 %) and 39.23 % with the mouse enzyme (PDB no. 7ODC). The crystal structure of the *T. brucei* enzyme obtained with bound cofactor PLP (PDB no. 1QU4 at 2.9 Å) was, therefore, used as template to build the PfODC homology model. Figure 1 shows the alignment between the 411 PfODC residues and *T. brucei* ODC used to create the model and also indicates the secondary structural elements for each protein.

The resulting homology model consisted of 373 residues based on the template structure plus an ab initio constructed 38 residue malaria-specific insert. The root-mean-square deviation (RMSD) value between the model carbon α-backbone and the *T. brucei* structure was 0.816 Å as determined by PROFIT. This value increased to 6.917 Å when the ab initio modeled insert of 38 residues was included in the comparison. The former value compares favorably to results of the 3DCrunch project, which showed that 63% of sequences sharing 40–49% identity with their template, yield models that deviate by <3 Å from control X-ray crystallography structures.[28] PROCheck analyses of the PfODC model, which included the 38 residue insert, produced a Ramachandran plot in which 84.2% of the residues were in the most favored regions (Fig. 2). Most of the main-chain and side-chain parameters were better than typical values allowed, and the rest of the parameters were within the allowed ranges. Quality analyses were also performed with the program WHAT_CHECK from the WHAT IF package, and several stereochemical parameters are summarized in Table I. From this table, the quality of both the monomeric and dimeric forms of PfODC seems as good as those of the reported *T. brucei* and *H. sapiens* structures with which it is compared.

The PfODC monomer consists of two distinct domains, an N-terminal α/β TIM barrel and a C-terminal modified Greek-key β-barrel [Fig. 3(A)]. These features correlate closely to all the other eukaryotic ODC structures characterized to date.[12–16] Evaluation of the relationships with the human ODC crystal structure (PDB no. 1D7K)[12]

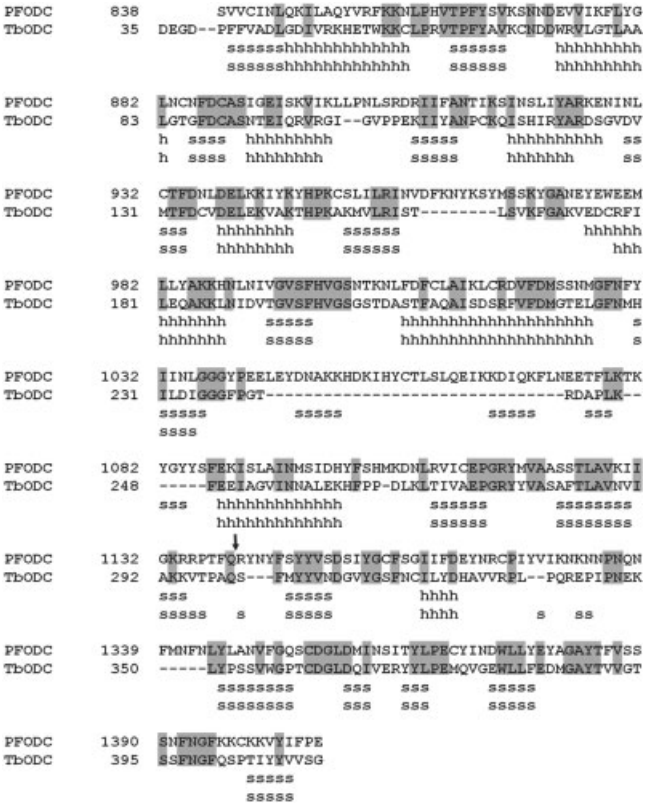

Fig. 1. Sequence alignment of *P. falciparum* ODC (PfODC) and the template used for homology modeling, *T. brucei* ODC (TbODC, PDB no. 1QU4) obtained with SIM using default parameters. Identical residues are shaded, and the secondary structural elements are indicated: s for β-sheets and h for α-helices. The site where the 158 residues malaria-specific insert was removed to create the PfODC model is indicated with an arrow.

indicates large similarities, especially in the structural motifs of the N-terminal α/β barrel and the C-terminal β-sheet[12] [Fig. 3(B)]. Superimposition of the PfODC monomer on the human ODC structure yields a RMSD of 0.80 Å (involving 1348 atoms) with the areas scoring the worst B-factors being the loops connecting the well-conserved structural elements of the core protein. These regions are mostly of low structural complexity (as indicated with the SEG program)[39] and are elongated in the malaria protein compared to other ODCs. Other studies have suggested that the low-complexity inserts found in malaria proteins encode for nonglobular domains that occur on the surface of proteins and are not involved in the functional folding of the proteins.[43] However, the 38-residue insert is predicted to have four antiparallel β-sheets (I1–I4) with the first two longer than the second pair and does not contain low complexity areas [Fig. 3(A)]. No firm conclusions are possible for the exact orientation of the bulk of the loop in space. In the model, the insert seems to lie parallel to the rest of the protein and to bulge out toward the C-terminal domain on the same side of the monomer as the entry to the active site. No significant interactions are apparent between the protein core and the insert. However, the insert is bridged by flexible Gly residues ($Gly_{1036\text{-}1038}$ and Gly_{1083}), which could act as hinge regions and allow mobility of the insert. The attachment site for the 158-amino acid insert, which was removed in PfODC to create the model, is in the C-terminal three quarters of the loop between C2b and C3 [Fig. 3(A)]. The junction region between the N- and C-terminal domains of eukaryotic ODCs (region 300–340 in the murine enzyme) varies in length from 40 residues for the mouse ODC to 115 residues for the closely related *E. coli* arginine decarboxylase enzyme.[44] The 158-residue insert in PfODC occurs in the equivalent region, suggesting a considerable tolerance for sequence length variations in this area and a probable species-specific property. It is likely that the inserted residues could be involved in the stabilization of ODC dimer interactions and/or the bifunctional AdoMetDC-ODC protein in the malaria parasite.

Dimeric PfODC

Eukaryotic ODC is an obligate homodimeric enzyme with two active sites at the interface between the two monomers.[1,45] The PfODC monomers were superimposed on the dimeric *T. brucei* crystal structure by using the improved fit module of SWISS-PdbViewer followed by energy minimization with Discover3 to create a dimeric structure of the malarial enzyme. Minimization was performed by using a conjugate gradient to a maximum derivative of 0.0030 after 10,000 iterations involving 1398 atoms with RMSD of 0.37 Å and energy of −15 350 kcal/mol. Convergence to a lower derivative was not obtained, probably because of the presence of the malaria-specific areas present as unconstrained loops on the surface of the protein. The RMSD values of the structures before and after minimization were 2.370 Å and 3.045 Å for the backbone and side-chain atoms, respectively. Analyses of the quality of the dimer as indicated with the WHAT IF program indicates a good working structure compared with the *T. brucei* and human structures (Table I).

The dimer is composed of a head-to-tail association of the two monomers, with the C-terminal domain of one monomer vertical to the N-terminal domain of the second monomer (Fig. 4). Several interactions between these two domains are apparent. As is the case in the *T. brucei* enzyme, the dimer interface of PfODC is characterized by an aromatic amino acid zipper.[13] Phe_{1392}, Tyr_{1305}, and Phe_{1319} (substituting a second Tyr residue found in *T. brucei*) are involved in hydrophobic contacts across the dimer interface, forming an antiparallel stacked interaction via their aromatic rings. A pronounced hydrophobic contact is predicted between Tyr_{1305} and Ile_{915} in an area that is well conserved in sequence identity in all ODCs but not in PfODC (residues 111–115: ANPCK; PfODC residues 912–916: ANTIK). A salt bridge (1.94 Å) is predicted between Asp_{1359} and Arg_{1134} from the opposite monomer as well as between Lys_{1133} and Glu_{1369} (1.85 Å). There are several stabilizing interactions close to the active site residues. Particularly for PfODC, Lys_{970} is predicted to interact with various residues surrounding the active site Cys_{1355} donated by the opposite monomer. Lys_{970} forms a hydrogen bond with Asp_{1356} and hydrophobic contacts

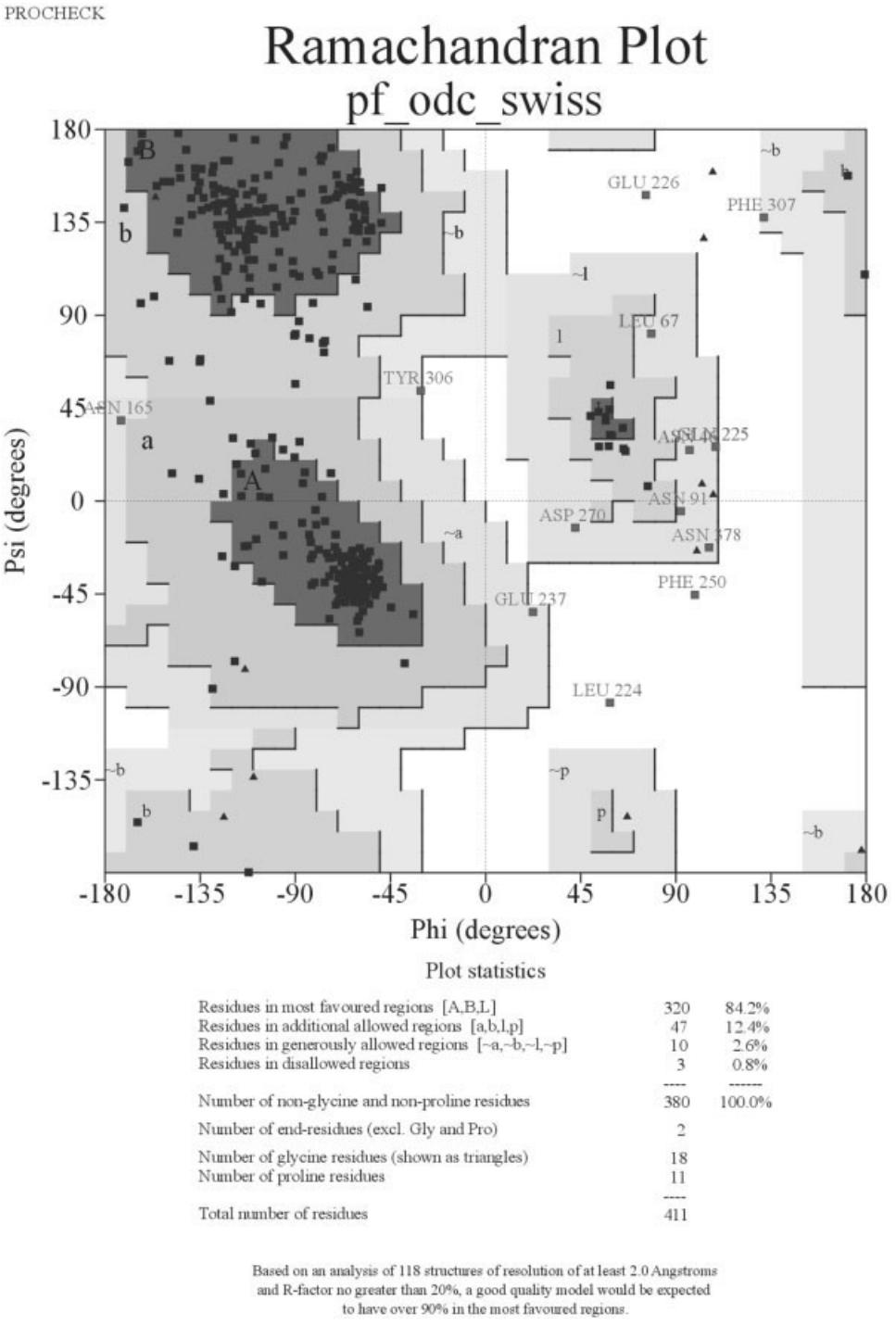

Fig. 2. Ramachandran plot for the model of PfODC produced by PROCHECK. 84.2% of the residues are present in favorable structural areas with the exception of three residues in disallowed regions (Glu, Leu, and Phe).

with Gly_{1357}, Asp_{1359}, and Gly_{1352}. Inactivation of PfODC after replacement of Asp_{1356}, Asp_{1359}, or Lys_{970} with alanine confirms the involvement of the latter amino acids in the dimerization of PfODC[46] and, therefore, provides experimental support for the predicted PfODC dimer structure.

Active Site Pocket of Dimeric PfODC

To analyze the active site pocket of PfODC, the binding of PLP and ornithine was simulated. Transition state structures for PLP bound to ornithine via a Schiff-base were used and minimized into the active site pocket to an

TABLE I. Summary of WHAT IF Quality Assessment Data

Structure	2nd-generation packing quality	Ramachandran plot appearance	χ^1/χ^2 rotamer normality	Backbone conformation	Bond lengths*	Bond angle variability*	Omega angle restraints*
1QU4	−2.231	−2.051	−1.848	−0.052	0.612	1.674	1.527
1D7K	−1.1	−1.2	−0.3	−0.6	0.753	1.791	2.360
PfODC:							
Monomer	−3.658	−0.762	0.263	−1.681	1.282	1.290	1.295
Dimer	−3.978	−0.807	0.283	−1.849	1.282	1.291	1.294

Data for the *T. brucei* (PDB no.1QU4) and *H. sapiens* (PDB no. 1D7K) ODC enzymes are compared with the monomeric and dimeric form of PfODC. Values are structure Z-scores with + better than normal. *RMS Z-scores should be close to 1.0.

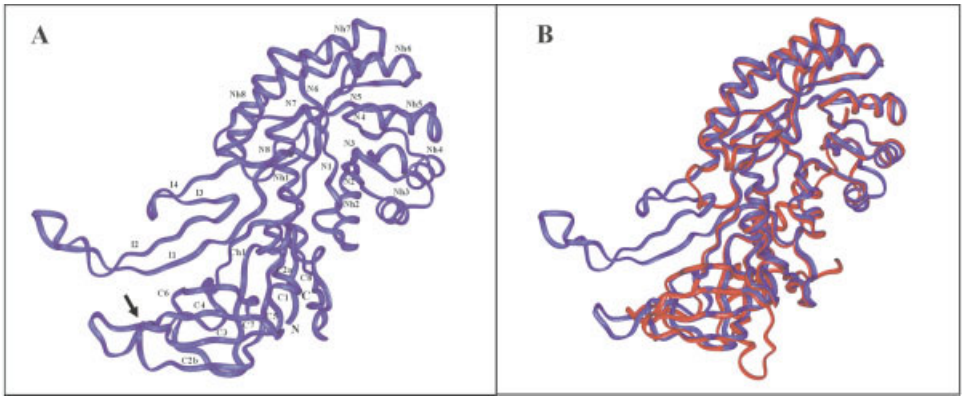

Fig. 3. Ribbon diagram of the homology model for the PfODC monomer (**A**) and in (**B**) compared with the human enzyme. A: The β-sheets are labeled in succession starting from the N-terminus (N1-N8, I1-I4, C1-C8), and the α-helices are specified in the N-terminal α/β-barrel domain (Nh1-Nh8). The site where the 158 residue malaria-specific insert was removed to create the PfODC model is indicated with an arrow. B: PfODC in blue is superimposed on the human ODC structure in red.

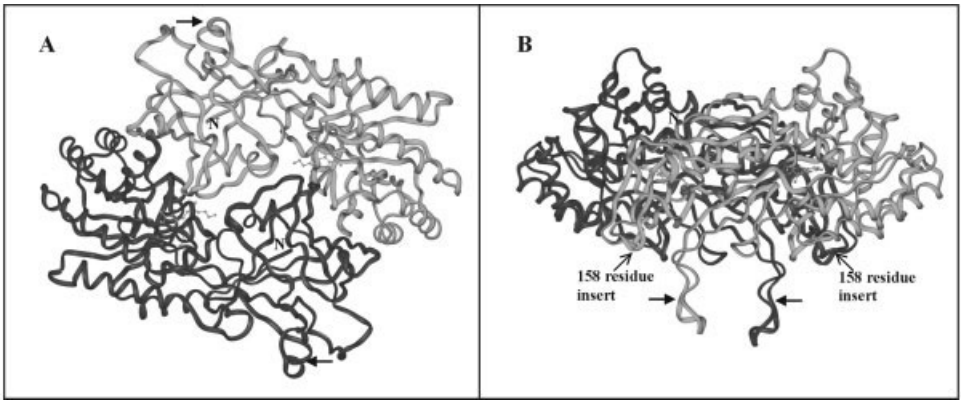

Fig. 4. Proposed dimeric form of PfODC. The two monomers are indicated in shades of gray, and the dimer is viewed from the bottom (**A**) and side (**B**). The PLP cofactor and DFMO inhibitor is indicated in ball-and-stick models in the two active site pockets formed at the interface between the two monomers. The N-terminus in each monomer is indicated. The location of the 158-residue insert removed to create the model in the protein is shown in (B). The filled arrows indicate the 38-residue insert that was modeled.

energy of −15 314 kcal/mol for the protein-ligand complex. Likewise, DFMO was bound to PLP via a Schiff-base but also covalently to Cys_{1355} (via S_γ) and minimized to −15 307 kcal/mol to further characterize the active site in binding to this substrate analog. The predicted PLP and substrate binding site of the PfODC has a few residues within 3.0 Å to enable hydrogen bonding and charge interactions (Fig. 5).

Possible residues interacting with either PLP, ornithine, or DFMO (as substrate analog) were identified by using LigPlot and are summarized in Table II. From these data it is clear that the active site residues are conserved

compared with the *T. brucei* and human enzymes in binding of PLP to Cys_{1355} (from the second monomer), $Asp_{887,}$ Arg_{955}, His_{998}, Ser_{1001}, Gly_{1037}, Glu_{1114}, Gly_{1116}, and Tyr_{1384}. However, residues $Thr_{933,}$ Met_{967}, and Asn_{1034} were present only in the PfODC PLP-binding site. The substrate-binding site was deduced from interactions with both ornithine and DFMO and consists of mutually conserved (compared with *T. brucei* and the human enzymes) residues Lys_{868}, $Asp_{1320,}$ Cys_{1355}, Asp_{1356}, $Tyr_{1384,}$ Phe_{1392}, and $Asn_{1393.}$ In the PfODC model, Cys_{1355} makes contact with Lys_{868} as well as Ala_{889} from the opposite monomer.

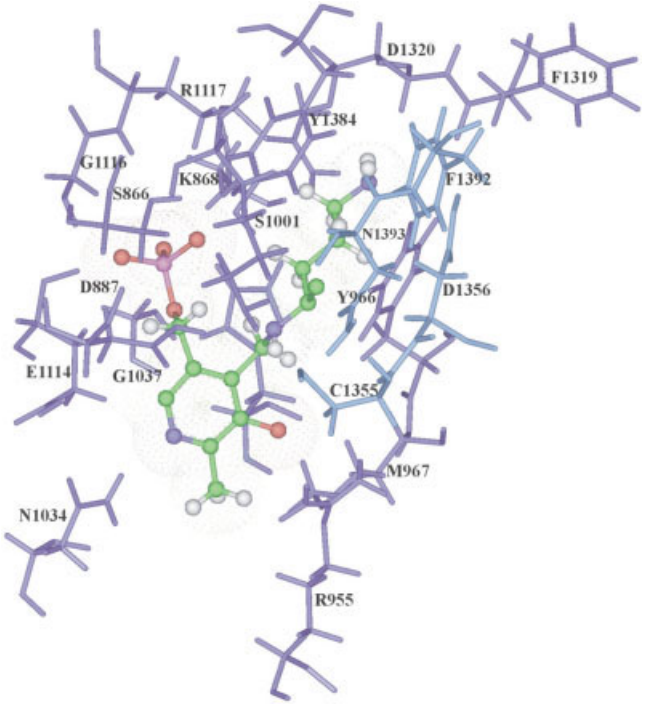

Fig. 5. Active site residues of the PfODC indicating the interactions with PLP and ornithine. PLP and Schiff-base linked ornithine are indicated in ball-and-sticks and with van der Waals surfaces shown. Residues are colored in different shades of blue indicating the contribution by the two respective monomers.

TABLE II. Active Site Residues Involved in Interactions With Ornithine as Substrate; DFMO as Inhibitor, or PLP as Cofactor

Ligand	*T. brucei* residues	*H. sapiens* residues	PfODC residues
PLP		Cys360	Cys1355A
	Arg154	Arg154	Arg955B
	Glu274	Glu274	Glu1114B
	Asp88	Asp88	Asp887B
	His197	His197	His998B
	Ala67	Ala67	Ser866B
	Tyr389	Tyr389	Tyr1384B
	Ser200		Ser1001B
	Gly276	Gly276	Gly1116B
	Arg277	Arg277	
	Gly236	Gly236	Gly1037B
	Gly237	Gly237	
			Thr933B
			Asn1034B
			Met967B
Substrate	Tyr389	Tyr389	Tyr1384B
	Cys360		Cys1355B
	Phe397	Phe397	Phe1392A
	Asp361		Asp1356A
	Tyr331		Phe1319B
	Asp332		Asp1320B
		Asn398	Asn1393A
		Val68	
		Ala67	
		Lys69	Lys868B
		Asn71	
		Glu94	
		Cys70	
		Ala392	
			Arg1117B
			Tyr966B

Active site residues were identified with LigPlot v 4.0 for the *T. brucei, H. sapiens,* and *P. falciparum* ODC enzymes. For PfODC, the numbering is according to the bifunctional enzyme complex, and A and B indicate which monomer contributed a residue toward the active site.

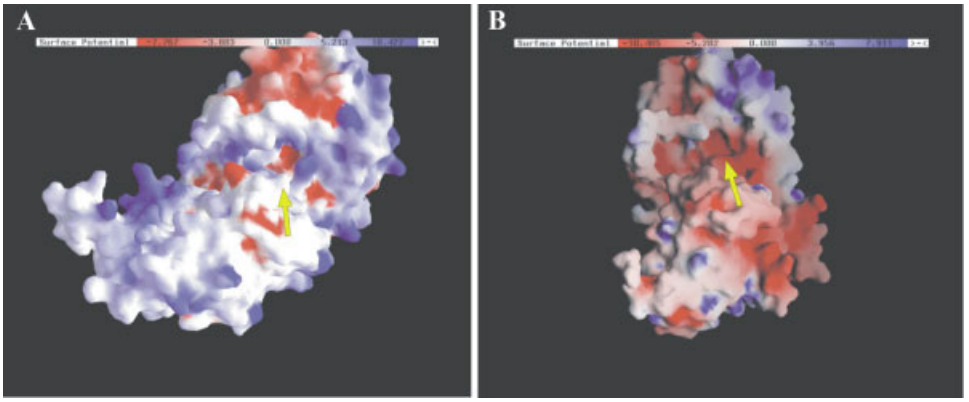

Fig. 6. Molecular surface potentials of the monomeric PfODC (**A**) and human ODC (**B**) structures. Surfaces were created with GRASP and are colored red and blue to distinguish between the most electrostatically negative and positive regions, respectively. Arrows indicate the view into the α/β-barrel and active site pocket.

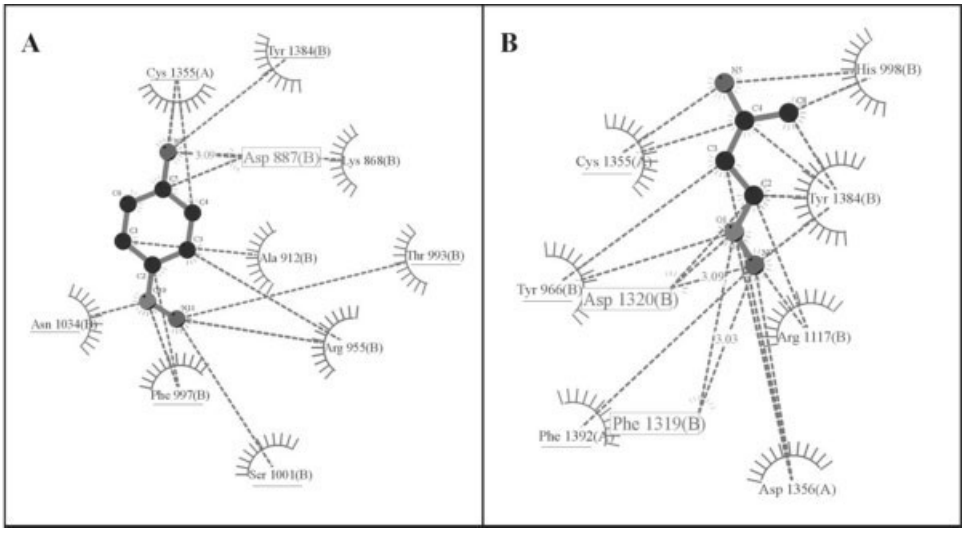

Fig. 7. Ligplot analyses of the interactions between two competitive inhibitors and PfODC. **A:** CGP52622A. **B:** CGP54169A. Hydrogen bonds and their lengths are indicated between the ligand and nonligand residues in blocks. Nonligand residues involved in hydrophobic contacts with the ligand are indicated in arcs with spokes. Residues in PfODC that are not involved in binding of the inhibitors to the human ODC are underlined.

As with the PLP-binding site, two residues (Tyr_{966} and Arg_{1117}) were only found in the PfODC substrate-binding site and not in either the human or *T. brucei*-binding sites. Of the five PfODC-specific residues characterizing the entire active site pocket of the malarial enzyme, only Thr_{933} and Arg_{1117} are conserved in comparison with the primary amino acid sequences of mammalian, *T. brucei* and *L. donovani*. The PfODC-specific residues Met_{967}, Asn_{1034}, and Tyr_{966} could have implications in the rational design of PfODC-specific lead inhibitors.

Single substitution of Lys_{868}, Lys_{970}, Cys_{1355}, or Asp_{1356} with alanine abolished enzyme activity, providing experimental support for the role of these residues in the activity of PfODC, whether through interactions with the substrate or cofactor (Lys_{868}, Asp_{1356}, and Cys_{1355}) or by disruption of interactions that stabilize the active dimer (Lys_{970} and Asp_{1356}).[46] The catalytic residues showed similar spatial orientations as those in the human structure. However, one interesting difference is the electrostatic potential at the surface of the active site pockets. PfODC has a very pronounced positively charged ring at the entrance to the negatively charged inner pocket, whereas this division is not as distinct for the human enzyme (Fig. 6). These dissimilar properties could have positive implications for the design of malaria-specific ODC inhibitors.

Docking of Various Ligands in the Active Site Pocket of PfODC

Inhibition of PfODC activity by DFMO occurs with a K_i of 87.6 $\pm$ 14.3 μM, almost double that of the murine enzyme.[47] To simulate the binding of the irreversible competitive inhibitor DFMO, the compound was covalently linked to the active-site Cys_{1355} (atom S_γ) as well as coupled to PLP via a Schiff-base. Analyses of the minimized interacting site of PfODC with DFMO indicated mutually conserved residues between the different species (Table II) and explains the nonspecific inhibition of ODC's by DFMO.[47]

Another series of potent ODC inhibitors were synthesized as analogs of 3-amino-oxy-1-propanamine.[48,49] Members of this series, CGP52622A and CGP54169A (Novartis Pharma), are reversible competitive inhibitors of PfODC with IC_{50} values of 63.5 nM and 25 nM, respectively.[47] Putative interactions of these inhibitors in the active site pocket of PfODC were analyzed by superimposing the structures on the coordinates of the corresponding ligands minimized in the PfODC active site pocket. Stable complexes had minimized energies of -15 343.94 kcal/mol for the CGP52622A-PfODC complex and a corresponding -15 346.68 kcal/mol for the CGP54169A-PfODC complex. LigPlot analyses of the interactions formed between the individual inhibitors and PfODC are shown in Figure 7. In CGP52622A, inhibition can be explained by its interaction with essential residues involved in binding of PLP (Asp_{887}, Arg_{955}, Thr_{933}, Ser_{1001}, Asn_{1034}, and Cys_{1355}) as well as substrate (Lys_{868}, Tyr_{1384}, and Cys_{1355}). Two additional interactions with Ala_{912} and Phe_{997} are also suggested. The calculated total free energy of interaction of this inhibitor with PfODC was -32.1 kcal/mol. As expected for a substrate analog, CGP54169A shows interactions with residues predicted to bind to ornithine (Arg_{1117}, Tyr_{966}, Phe_{1319}, Asp_{1320}, Asp_{1356}, Cys_{1355}, and Phe_{1392}) and also to two PLP-binding residues (His_{998} and Tyr_{1384}) with a total free energy of the interactions of -27.67 kcal/mol. This is slightly lower than the binding free energy of -84.2 kcal/mol obtained for the interactions with Schiff-base linked PLP-ornithine as natural ligands.

The CGP series of compounds inhibit rat liver ODC with IC_{50} values in the nanomolar range and recombinantly expressed human ODC with IC_{50} values of 25 and 10 nM for CGP52622A and CGP54169A, respectively (R. Walter,

personal communication).[48,49] Similar analyses as described above were conducted on the active site pocket of human ODC (PDB no. 1D7K) to identify the interacting sites of CGP54169A and CGP52622A. Stable complexes were minimized to energies of −14 821 kcal/mol for the CGP52622A-human ODC complex and −14 807.75 kcal/mol for the CGP54169A-human ODC complex. The predicted interaction sites of CGP52622A with the human ODC did not include Thr_{933}, Ser_{1001}, $Asn_{1034,}$ Cys_{1355}, Tyr_{1384}, and Ala_{912} (PfODC numbering) shown to be involved in its interaction with PfODC (Fig. 7). The total calculated free energy of the interaction between CGP52622A and the human ODC was −27.07 kcal/mol. Furthermore, CGP54169A-human ODC interactions also excluded residues Tyr_{966}, Cys_{1355}, and Phe_{1392} of PfODC (Fig. 7) with a calculated free energy for the complex of −26.6 kcal/mol. Again, the interaction of the natural ligands, PLP and ornithine, with human ODC has a somewhat higher free binding energy of −71.9 kcal/mol. Importantly, Cys_{1355} is essential to ODC activity,[1,2,11,46] and both inhibitors bind this residue in PfODC but not the equivalent residue of the human enzyme. Furthermore, Thr_{933}, Phe_{997}, and Tyr_{966} uniquely interact with the inhibitors only in the malarial enzyme. The proposed interactions of the inhibitors with the essential active site binding residues would, therefore, prevent or interfere with any subsequent binding of the substrate/cofactor and lead to significant PfODC inhibition. Taken together, the marked inhibition of PfODC seen with the CGP compounds can be explained by their interaction with parasite-specific residues, including the essential Cys_{1355}. These compounds further aid in the mapping of the PfODC active site pocket and could act as scaffolds in the design of differential PfODC inhibitors.

CONCLUSION

The homology model of PfODC presented here is supported in several important aspects by published mutagenesis results. It provides a valuable resource to guide further studies to confirm the validity of the model and to explain structure-function relationships. Species-specific differences between PfODC and the human enzyme were observed in the active site pocket and at the dimerization interface. The elucidation of the active site residues involved in PfODC and their interactions with substrate/cofactor analogs paves the way toward the design of improved and parasite-specific inhibitors. The PfODC model also provides explanations for the low K_i values seen for the CGP52622A and CGP54169A inhibitors and supports the further evaluation of these compounds as possible antimalarial agents. Mutational studies are in progress to confirm the parasite-specific properties revealed by the PfODC homology model. The characterization of the structural properties of the malarial ODC is the first step in a structure-based approach for the design of novel and malaria-specific inhibitors that could be clinically useful.

ACKNOWLEDGEMENTS

A.I. Louw and L. Birkholtz hold a Mellon Foundation Mentoring Fellowship (Andrew F. Mellon Foundation, New York, NY). We thank Dr. C. Kenyon for helpful discussions and Prof. R.D. Walter for the chemical structures of the CGP inhibitors and the IC_{50} values of recombinantly expressed human ODC.

REFERENCES

1. Cohen SS. A guide to the polyamines. New York: Oxford University Press; 1998.
2. McCann PP, Pegg AE. Ornithine decarboxylase as an enzyme target for therapy. Pharmacol Ther 1992;54:195–215.
3. Marton LJ, Pegg AE. Polyamines as targets for therapeutic intervention. Annu Rev Pharmacol Toxicol 1995;35:55–91.
4. Wang CC. Molecular mechanisms and therapeutic approaches to the treatment of African trypanosomiasis. Annu Rev Pharmacol Toxicol 1995;35:93–127.
5. Assaraf YG, Golenser J, Spira DT, Bachrach U. Polyamine levels and the activity of their biosynthetic enzymes in human erythrocytes infected with the malaria parasite, *Plasmodium falciparum*. Biochem J 1984;222:815–819.
6. Assaraf YG, Golenser J, Spira DT, Messer G, Bachrach U. Cytostatic effect of DL-αμdiflouromethylornithine against *Plasmodium falciparum* and its reversal by diamines and spermidine. Parasitol Res 1987b;73:313–318.
7. Bitoni AJ, McCann PP, Sjoerdsma A. *Plasmodium falciparum* and *Plasmodium berghei*: effects of ornithine decarboxylase inhibitors on erythrocytic schizogony. Exp Parasitol 1987;64:237–243.
8. Bitonti AJ, Dumont JA, Bush TL, Edwards ML, Stemerick DM, McCann PP, Sjoerdsma A. Bis(benzyl)polyamine analogs inhibit the growth of chloroquine- resistant human malaria parasites (Plasmodium falciparum) in vitro and in combination with alpha-difluoromethylornithine cure murine malaria. Proc Natl Acad Sci USA 1989;86:651–655.
9. Wright PS, Cross-Doersen DE, Schroeder KK, Bowlin TL, McCann PP, Bitonti AJ. Disruption of Plasmodium falciparum-infected erythrocyte cytoadherence to human melanoma cells with inhibitors of glycoprotein processing. Biochem Pharmacol 1991;41:1855–1861.
10. Muller S, Da'dara A, Luersen K, Wrenger C, Das Gupta R, Madhubala R, Walter RD. In the human malaria parasite Plasmodium falciparum, polyamines are synthesized by a bifunctional ornithine decarboxylase, S-adenosylmethionine decarboxylase. J Biol Chem 2000;275:8097–8102.
11. Pegg AE. Characterisation of ornithine decarboxylase from various sources. In: Hayashi S, Hayashi S, editors. Ornithine decarboxylase: biology, enzymology and molecular genetics. Oxford, England: Pergamon Press, Inc.; 1989. p 21–28.
12. Almrud JJ, Oliveira MA, Kern AD, Grishin NV, Phillips MA, Hackert ML. Crystal structure of human ornithine decarboxylase at 2.1 A resolution: structural insights to antizyme binding. J Mol Biol 2000;295:7–16.
13. Grishin NV, Osterman AL, Brooks HB, Phillips MA, Goldsmith EJ. X-ray structure of ornithine decarboxylase from Trypanosoma brucei: the native structure and the structure in complex with alpha-difluoromethylornithine. Biochemistry 1999;38:15174–15184.
14. Momany C, Ernst S, Ghosh R, Chang NL, Hackert ML. Crystallographic structure of a PLP-dependent ornithine decarboxylase from Lactobacillus 30a to 3.0 A resolution. J Mol Biol 1995;252:643–655.
15. Vitali J, Carroll D, Chaudhry RG, Hackert ML. Three-dimensional structure of the Gly121Tyr dimeric form of ornithine decarboxylase from Lactobacillus 30a. Acta Crystallogr D Biol Crystallogr 1999;55:1978–1985.
16. Kern AD, Oliveira MA, Coffino P, Hackert ML. Structure of mammalian ornithine decarboxylase at 1.6 A resolution: stereochemical implications of PLP-dependent amino acid decarboxylases. Struct Fold Des 1999;7:567–581.
17. Ekstrom JL, Mathews II, Stanley BA, Pegg AE, Ealick SE. The crystal structure of human S-adenosylmethionine decarboxylase at 2.25 A resolution reveals a novel fold. Struct Fold Des 1999;7:583–595.

18. Baca AM, Hol WG. Overcoming codon bias: a method for high-level over-expression of Plasmodium and other AT-rich parasite genes in *Eschericia coli*. Int J Parasitol 2000;30:113–118.
19. Chang SP. Expression systems to best mimick the native structure. Am J Trop Med Hyg 1994;50:20–26.
20. Srinivasan N, Guruprasad K, Blundell TL. Comparative modelling of proteins. In: Sternberg MJE, Sternberg MJE, editors. Protein structure prediction: a practical approach. Oxford: Oxford University Press; 1996.
21. Lemcke T, Christensen IT, Jorgensen FS. Towards an understanding of drug resistance in malaria: three-dimensional structure of Plasmodium falciparum dihydrofolate reductase by homology building. Bioorg Med Chem 1999;7:1003–1011.
22. Toyoda T, Brobey RK, Sano G, Horii T, Tomioka N, Itai A. Lead discovery of inhibitors of the dihydrofolate reductase domain of Plasmodium falciparum dihydrofolate reductase-thymidylate synthase. Biochem Biophys Res Commun 1997;235:515–519.
23. Warhurst DC. Antimalaria drug discovery: development of inhibitors of dihydrofolate reductase active in drug resistance. Drug Discov Today 1998;3:538–546.
24. Rastelli G, Sirawaraporn W, Sompompisut P, Vilaivan T, Kamchonwongpaisan S, Ouarrel R, Lowe G, Thebtaranonth Y, Yuthavong Y. Interaction of pyrimethamine, cycloguanil, WR99210 and their analogues with *Plasmodium falciparum* dihydrofolate reductase: structural basis of antifolate resistance. Bioorg Med Chem 2000;8:1117–1128.
25. Thompson JD, Higgins DG, Gibson TJ. CLUSTAL W: improving the sensitivity of progressive multiple sequence alignment through sequence weighting, position-specific gap penalties and weight matrix choice. Nucleic Acids Res 1994;22:4673–4680.
26. Guex N, Peitsch MC. SWISS-MODEL and the Swiss-PdbViewer: an environment for comparative protein modeling. Electrophoresis 1997;18:2714–2723.
27. Guex N, Diemand A, Peitsch MC. Protein modelling for all. Trends Biochem Sci 1999;24:364–367.
28. Guex N, Peitsch MC. Molecular modelling of proteins. Immunol News 1999;6:132–134.
29. Peitsch MC, Tschopp J. Comparative molecular modelling of the Fas-ligand and other members of the TNF family. Mol Immunol 1995;32:761–772.
30. Peitsch MC. Protein modelling by E-mail. Bio/Technology 1995;13:658–660.
31. Peitsch MC. ProMod and Swiss-Model: internet-based tools for automated comparative protein modelling. Biochem Soc Trans 1996;24:274–279.
32. Peitsch MC, Herzyk P, Wells TN, Hubbard RE. Automated modelling of the transmembrane region of G-protein coupled receptor by Swiss-model. Receptors Channels 1996;4:161–164.
33. Huang X, Miller W. A time-efficient linear-space local similarity algorithm. Adv Appl Math 1991;12:337.
34. Vriend G. WHAT IF: a molecular modelling and drug design program. J Mol Graph 1990;8:52–56.
35. Laskowski RA, MacAthur MW, Moss DS, Thorton JM. PROCHECK: a program to check the stereochemical quality of protein structures. J Appl Crystallogr 1993;29:283–291.
36. Nicholls A, Sharp KA, Honig B. Protein folding and association: insights from the interfacial and thermodynamic properties of hydrocarbons. Proteins 1991;11:281–296.
37. Orengo CA, Michie AD, Jones S, Jones DT, Swindells MB, Thorton JM. CATH: a hierarchic classification of protein domain structures. Structure 1997;5:1093–1108.
38. Murzin AG, Brenner SE, Hubbard T, Chothia C. SCOP: a structural classification of proteins database for the investigation of sequences and structures. J Mol Biol 1995;247:536–540.
39. Wooton JC, Federhen S. Analysis of compositionallz baised regions in sequence databases. Methods Enzymol 1996;266:554–571.
40. Wallace AC, Laskowski RA, Thorton JM. LIGPLOT: a program to generate schematic diagrams of protein-ligand interactions. Protein Eng 1995;8:127–134.
41. Coleman CS, Stanley BA, Pegg AE. Effects of mutations at active site residues on the activity of ornithine decarboxylase and its inhibition by active site directed irreversible inhibitors. J Biol Chem 1993;268:24572–24579.
42. Osterman A, Grishin NV, Kinch LN, Phillips MA. Formation of functional cross-species heterodimers of ornithine decarboxylase. Biochemistry 1994;33:13662–13667.
43. Pizzi E, Frontali C. Low-complexity regions in *Plasmodium falciparum* proteins. Genome Res 2001;11:218–229.
44. Osterman AL, Lueder DV, Quick M, Myers D, Canagarajah BJ, Phillips MA. Domain organization and a protease-sensitive loop in eukaryotic ornithine decarboxylase. Biochemistry 1995;34:13431–13436.
45. Pegg AE, Shantz LM, Coleman CS. Ornithine decarboxylase: structure, function and translational regulation. Biochem Soc Trans 1994;22:846–852.
46. Wrenger C, Luersen K, Krause T, Muller S, Walter RD. The Plasmodium falciparum bifunctional ornithine decarboxylase, S-adenosylmethionine decarboxylase enables a well balanced polyamine synthesis without domain-domain interaction. J Biol Chem 2001;276:29651–29656.
47. Krause T, Luersen K, Wrenger C, Gilberger TW, Muller S, Walter RD. The ornithine decarboxylase domain of the bifunctional ornithine decarboxylase/S-adenosylemethionine decarboxylase of *Plasmodium falciparum*: recombinant expression and catalytic properties of two different constructs. Biochem J 2000;352:287–292.
48. Mett H, Standek J, Lopez-Ballester JA, Janne J, Alhonene L, Sinervirta R, Frei J, Renegrass U. Pharmacological properties of the ornithine decarboxylase inhibitor 3-aminooxy-1-propanamine and several structural analogues. Cancer Chemother Pharmacol 1993;32:39–45.
49. Standek J, Frei J, Schneider P, Regenass U. 2-Substituted 3-(aminoozy)propanamines as inhibitors of ornithine decarboxylase: synthesis and biological activity. J Med Chem 1992;35:1339–1344.